Published in final edited form as:

Neurobiol Dis. 2015 October ; 82: 22–31. doi:10.1016/j.nbd.2015.04.018.

Survival benefit and phenotypic improvement by hamartin gene therapy in a tuberous sclerosis mouse brain model

Shilpa Prabhakar[a], **Xuan Zhang**[a], **June Goto**[b], **Sangyeul Han**[c], **Charles Lai**[a], **Roderick Bronson**[d], **Miguel Sena-Esteves**[e], **Vijaya Ramesh**[c], **Anat Stemmer-Rachamimov**[f], **David J. Kwiatkowski**[b,*], and **Xandra O. Breakefield**[a,*]

[a]Molecular Neurogenetics Unit, Department of Neurology and Center for Molecular Imaging Research, Department of Radiology, Massachusetts General Hospital, and Program in Neuroscience, Medical School, Boston, MA, USA

[b]Translational Medicine Division, Department of Medicine, Brigham and Women's Hospital, Harvard Medical School, Boston, MA, USA

[c]Center for Human Genetic Research, Massachusetts General Hospital, Boston, MA, USA

[d]Rodent Histopathology Core Facility, Harvard Medical School, Boston, MA, USA

[e]Neurology Department, Gene Therapy Center, University of Massachusetts Medical School, Worcester, MA, USA

[f]Department of Pathology, Massachusetts General Hospital, Boston, MA, USA

Abstract

We examined the potential benefit of gene therapy in a mouse model of tuberous sclerosis complex (TSC) in which there is embryonic loss of Tsc1 (hamartin) in brain neurons. An adeno-associated virus (AAV) vector (serotype rh8) expressing a tagged form of hamartin was injected into the cerebral ventricles of newborn pups with the genotype $Tsc1^{cc}$ (homozygous for a conditional floxed Tsc1 allele) SynI-cre+, in which Tsc1 is lost selectively in neurons starting at embryonic day 12. Vector-treated *$Tsc1^{cc}SynIcre^{+}$* mice showed a marked improvement in survival from a mean of 22 days in non-injected mice to 52 days in AAV hamartin vector-injected mice, with improved weight gain and motor behavior in the latter. Pathologic studies showed normalization of neuron size and a decrease in markers of mTOR activation in treated as compared to untreated mutant littermates. Hence, we show that gene replacement in the brain is an effective therapeutic approach in this mouse model of TSC1. Our strategy for gene therapy has the advantages that therapy can be achieved from a single application, as compared to repeated treatment with drugs, and that AAV vectors have been found to have minimal to no toxicity in clinical trials for other neurologic conditions. Although there are many additional issues to be addressed, our studies support gene therapy as a useful approach in TSC patients.

*Corresponding authors: David J. Kwiatkowski, MD, Ph.D., Pulmonary Medicine Division, Brigham and Women's Hospital, 1 Blackfan Circle, Room 6-213, Boston, MA 02115 USA Phone:617-355-9005, Fax:617-355-9016, dk@rics.bwh.harvard.edu; Xandra O. Breakefield, Ph.D., Molecular Neurogenetics Unit, Massachusetts General Hospital-East, 13th Street, Building 149, Charlestown, MA 02129 USA, Phone 617-726-5728, Fax 617-724-1537, breakefield@hms.harvard.edu.

Conflict of interest

The authors declare that they have no conflict of interest.

Keywords

Tuberous Sclerosis Complex; TSC; TSC1; TSC2; gene therapy; AAV; neuron

Introduction

Tuberous sclerosis complex (TSC) is an autosomal dominant disease caused by mutations in *TSC1* or *TSC2,* genes which encode hamartin and tuberin, respectively (Crino, 2013; Kwiatkowski et al., 2010). These proteins are critical in modulating the activity of mTOR which, in turn, regulates development and growth of many tissues (Laplante and Sabatini, 2012). Benign tumors develop in the heart, brain, kidneys, skin, and lungs in TSC patients, and typically follow the classic Knudsen model in which there is a subsequent mutation in the corresponding normal allele ('second hit') occurring in somatic cells resulting in complete loss of either TSC1 or TSC2 expression in cells throughout the body. Neurologic symptoms are seen in over 90% of TSC patients, and include epilepsy, autism spectrum disorders, intellectual disability, attention deficit-hyperactivity, anxiety and sleep disorders (Jülich and Sahin, 2013). Central nervous system (CNS) pathology in TSC includes cortical tubers (focal cortical lesions with giant cells), disorganized architecture with loss of layers in cortical migration tracts, enlarged neurons, reduced myelination and impaired neuronal connectivity (Crino, 2013; Jülich and Sahin, 2013). In addition, subependymal giant cell astrocytomas (SEGAs) can develop from subependymal nodules, leading to hydrocephalus. Drugs that inhibit mTORC1, e.g. rapamycin and everolimus, have been shown to provide substantial clinical benefit for treatment of SEGAs (Franz et al., 2006; Franz et al., 2013), and may have benefit for seizure control (Krueger et al., 2013).

Insights into the pathophysiology and potential drug treatments for TSC have been achieved using a variety of rat and mouse models. Models include the Eker rat with a germ line mutation in *Tsc2* (Yeung, 2004), conditional floxed *Tsc1* and *Tsc2* mouse alleles which can be crossed with transgenic mice bearing (non-inducible or inducible) Cre recombinase under different cell-specific promoters, which are active, for example, in astrocytes (Uhlmann et al., 2002), neural progenitor cells (Carson et al., 2012; Anderl et al., 2011), and early neurons (Meikle et al., 2007). Other stochastic models have been achieved by electroporation of a Cre expression cassette into floxed neonatal mouse brains (Feliciano et al., 2013) or intracerebral ventricular (ICV) injection of an adeno-associated virus (AAV) vector encoding Cre into newborn floxed mice (Prabhakar et al., 2013). In these models many of the neurologic features of TSC are recapitulated including enlarged, dysplastic neurons, clusters of cells expressing both neuronal and glial markers, subependymal nodules, activation of the mTOR pathway, and decreased myelination. Neuropathological abnormalities in the mouse model used in this study in which transgenic animals expression Cre under the synapsin I promoter are crossed with mice bearing a floxed Tsc1 allele ($Tsc1^{cc}SynIcre^{+}$) include enlarged, dysplastic neurons and decreased myelination, and these mice die early apparently due to acute respiratory failure caused by seizures (Meikle et al., 2007). Most of these TSC mouse brain models have reduced body weight, tremor, hunched posture, seizures and motor abnormalities, with median survival varying from 0 to 180 days. Continuous treatment with rapamycin and analogues that block mTOR activity have been

shown to lead to dramatic survival benefit in several models, with a decrease in neural cell size, increased myelination, decreased seizures and improved behavior (Anderl et al., 2011; Meikle et al., 2008; Carson et al., 2012; Zeng et al., 2008). This drug benefit persists for a short while after treatment is ended, but then severe symptoms reappear followed by death.

Gene therapy for neurologic diseases is showing great promise (for review see Simonato et al., 2013; Nagabhushan Kalburgi et al., 2013; Maguire et al., 2014). In particular, AAV vectors have proven non-toxic in the context of the nervous system in mouse models, non-human primates and human clinical trials for a number of diseases. AAV vectors can be generated with capsids of different serotypes, with many showing widespread gene delivery to the brain after ICV (Gholizadeh et al., 2013; Broekman et al., 2006) or intravascular (IV) delivery (Yang et al., 2014a; Samaranch et al., 2012; Schuster et al., 2014), especially in neonatal and juvenile mice, with transgene expression persisting for years in non-dividing cells, such as neurons.

In this study we evaluated the therapeutic potential of gene replacement using neonatal ICV delivery of an AAV vector in a conditional *Tsc1* floxed model in which most neurons are depleted of hamartin from embryonic day 12 (Meikle et al., 2007). We demonstrate functional activity of the vector-encoded hamartin in cultured cells, expression throughout the brain following a single ICV injection of the AAV vector at P0, and marked increase in weight gain, normalization of motor behavior and prolonged survival in the AAV-hamartin-treated *Tsc1* floxed mice, comparable to that reported for ongoing rapamycin treatment in this model (Meikle et al., 2008). This recovery was accompanied by normalization of neural cell size and reduced levels of phospho-S6 (pS6) in the brains of vector-treated mutant mice. Advantages of a gene replacement approach using AAV include the possible effectiveness of only a single injection of vector and the low toxicity and extensive biodistribution of this vector. Since TSC1/hamartin is thought to function largely, if not exclusively, in a complex with TSC2/tuberin and TBC1D7 (Dibble et al., 2012), some overexpression of hamartin should have no adverse effects.

Methods

AAV vector design and packaging

An AAV vector plasmid, AAV-CMV-hamartin-cmyc (Fig. 1) was derived from the plasmid AAV-CBA-BGHpA (M.S-E.; Broekman et al., 2006). This plasmid carries two AAV2 ITR elements, one wild-type and one in which the terminal resolution site has been deleted, generating a vector that is packaged as a double-stranded (self-complementary) molecule. The AAV-CMV-hamartin-cmyc plasmid was generated by replacing the chicken beta actin (CBA) promoter in the parent plasmid with a PCR-amplified cytomegalovirus (CMV) promoter using a lentivirus vector construct (CSCW-IG; Sena-Esteves et al., 2004) as a template and the following primers: CMV-1: AAAGGTACCGATTAATAGTAATCAATTACGGGGT and CMV-2: AGCGCTAGCGGATCTGACGGTTCACT. This PCR product was inserted between KpnI and NheI sites in the plasmid. Human hamartin cDNA was PCR amplified using the original human hamartin plasmid TSC1-FLAGpcDNA (12–16; V.R.) as a template and the following primers: hamartin-1: AAAGCTAGCGCCACCATGGCCCAACAAGCAAATGTCGGGGA

and hamartin-2: AAAAGCGGCCGCTTAGCTGTGTTCATGATGAGTCTCATTG. The cmyc epitope was added onto hamartin by using the following primer: hamartin-cmyc: AAGCGGCCGCTCACAGGTCCTCCTCGCTGATCAGCTTCTGCTCGCTGTGTTCATG AT GAGTCTCATTG. This PCR product was inserted between NotI and SacI sites to generate the AAV-CMV-hamartin-cmyc plasmid. The AAV-CBA-GFP plasmid (Broekman et al., 2006) was provided by Dr. Bakhos Tannous (Mass. General Hospital). Both AAV vectors carried the bovine growth hormone polyadenylation signal at the 3′ end of the coding sequence. The fidelity of all PCR amplified sequences within the plasmids was confirmed by sequencing.

AAVrh8 serotype vectors were produced by transient co-transfection of 293T cells with calcium phosphate precipitation of vector plasmid (AAV-CMV-hamartin-cmyc or AAV-CBA-GFP), adenoviral helper plasmid pFΔ6, and a plasmid encoding the AAVrh8 capsid (pAR-rh8), as previously described (Broekman et al., 2006). Briefly, AAV vectors were purified by iodixanol gradient centrifugation followed by column chromatography using HiTrapQ anion exchange columns (GE Healthcare Life Sciences, Piscataway, NJ). The virus-containing fractions were concentrated using Centricon 100 kDa MWCO centrifugal devices (EMD Millipore, Billerica, MA) and the titer [genome copies (g.c.)/ml] was determined by real-time PCR amplification with primers and probe specific for the bovine growth hormone polyadenylation signal.

Cell culture, transfection and immunoblotting

293T human embryonic kidney (HEK) fibroblasts (obtained from Dr. David Baltimore, MIT) were maintained in high glucose DMEM (Cellgro, Manassas, VA) containing 10% fetal bovine serum (Sigma-Aldrich, St. Louis, MO) and 1% penicillin/streptomycin (Cellgro). Mouse neuronal cultures (obtained from Dr. Daniel Joyner, Department of Neurology, Alzheimer's Disease Research Unit, MGH, Charlestown, MA) were cultured as described (Stoothoff et al., 2009). Cells were maintained at 37°C in a humidified atmosphere of 5% CO_2 and 95% air. 293T cells were transfected with AAV-CMV-hamartin-cmyc, AAV-CBA-GFP, or TSC1 FLAG pcDNA3 (Murthy et al., 2000) plasmids using Lipofectamine 2000, following the manufacturer's protocol (Invitrogen, Carlsbad, CA). Seventy-two h later the transfected cells were scraped and cell lysates were prepared using radio-immunoprecipitation assay (RIPA) lysis buffer containing protease inhibitors (complete, Mini, Roche Diagnostics, Indianapolis, IN), followed by immunoblot analysis. Proteins were separated by electrophoresis in 10% Bis-Tris gels (Invitrogen) and transferred onto trans-Blot nitrocellulose membranes (Fisher Scientific, Lafayette, CO). Coomassie staining of gels was carried out to confirm that the samples were loaded equally. The membranes were blocked in 5% nonfat dry milk in PBS, pH 7.4, with 0.1% Tween 20 (PBS-Tween) for 1 h at room temperature. Primary antibodies, anti-C-Myc Peroxidase Conjugate (Sigma) or anti-hamartin polyclonal antibody (alphaHF3) (Haddad et al., 2002) were diluted in blocking solution and membranes were incubated overnight at 4°C or 1 h at room temperature, respectively. The blots were washed in PBS-Tween and then incubated for 1 h at room temperature in horseradish peroxidase (HRP)-conjugated secondary antibodies (Invitrogen). Reactive proteins were visualized using SuperSignal West Pico chemiluminescence reagent (Pierce, Rockford, IL) and exposure to X-ray film (BioMax MR, Kodak, St. Louis, MO]).

All immunoblots shown in one row of a figure are from the same gel-blot-exposure (Han et al., 2012).

S6K reporter assay

To evaluate the functional activity of hamartin-cmyc expressed by the AAV vector construct (AAV-CMV-hamartin-cmyc), we co-expressed HA-S6 kinase (HA-S6K), which is one of the direct substrates of mTORC1, in 293T cells (Han et al., 2012). The flag-tagged TSC1 in mammalian expression vector pcDNA3 (TSC1-FLAG) was used as a positive control. Briefly, at 20 h post-transfection, 293T cells were harvested and lysed in 0.5% NP-40 lysis buffer containing 150 mM NaCl, 50 mM Tris (pH 7.4), 50 mM NaF, 1 mM Na orthovanadate, 2 mM EDTA, and 1X Complete protease inhibitor cocktail (Roche). Cell lysates (500 μg) were then subjected to immunoprecipitation (IP) using anti-HA antibody (Covance, Berkeley, CA). Anti-HA immunoprecipitates or cell lysates were separated by 4–15% gradient SDS-PAGE (Bio-Rad, Hercules, CA) and probed with various antibodies, including anti-HA, anti-pS6K (T389) (Cell Signaling, Danvers, MA), anti-C-Myc (9E10, Developmental Studies Hybridoma Bank Iowa), or anti-FLAG (Sigma) antibodies.

Animals

Experimental research protocols were approved by the Institutional Animal Care and Use Committee (IACUC) for the Massachusetts General Hospital (MGH) following the guidelines of the National Institutes of Health for the Care and Use of Laboratory Animals. Experiments were performed on litters of mice with genotypes $Tsc1^{cc}SynIcre^{+}$ (mutant) and $Tsc1^{cw}SynIcre^{+}$ (normal) derived from matings of $Tsc1^{cw}SynIcre^{++}$ mice with $Tsc1^{cc}$ mice (Meikle et al., 2007). In addition, these mice carried the Cre-inducible ROSA26 *lacZ* marker allele (Mao et al., 1999; Meikle et al., 2007).

DNA analyses

DNA was prepared from mouse toes/tails by standard procedures for genotyping. Genotyping at the *Tsc1* gene was performed using a 4 primer system that allows simultaneous analysis of the *c, w*, and – alleles, followed by agarose gel electrophoresis (Meikle et al., 2005). Primers that amplify a 500 bp portion of the Cre recombinase gene were used to assess the presence of the *SynICre* allele (Meikle et al., 2005).

ICV injections

For vector injections, on the day of birth (P0), neonates were cryo-anesthetized and injected with 2 μl viral vector into each cerebral lateral ventricle with a glass micropipette (70–100 μm diameter at the tip) using a Narishige IM-300 microinjector at a rate of 2.4 psi/s (Narishige International, East Meadow, NY). The viral vector solution consisted of 2×10^{10} g.c. in 2 μl. Mice were then placed on a warming pad and returned to their mothers after regaining normal color and full activity typical of newborn mice. Mice were euthanized when they showed a weight loss of >15%, greatly reduced movement or other signs of distress.

Behavioral tests for mice

Behavioral tests were performed twice weekly by an observer blinded to genotype and treatment status of the mice. This included assessment of hind leg clasping behavior when suspended by the tail, scored as absent (0) or present (1); whole body tremor assessed by placing the palm of the hand on the back of the mouse, scored on a scale from absent (0) to severe and persistent (5); kyphosis (exaggerated rounding of the back), scored as absent (0) or present (1); and tail position observed during a 3 minute interval during which the animal was allowed to walk freely in a confined space, scored as normal (0), held horizontal (1), held above horizontal (2), or Straub position (elevated highly, 3) (Meikle et al., 2008).

Histology and immunohistochemistry (IHC)

For standard histology mouse brains were prepared after euthanasia with CO_2 by immediate removal of brains and 2–4 days of fixation in Bouin's solution (VWR International, Radnor, PA). Following paraffin embedding, 5 μm sections were cut and stained with either haematoxylin and eosin (H&E) or were used for IHC. IHC was performed using antigen retrieval in citrate buffer (pH 6) followed by staining with the EnVision System (Dako, Carpinteria, CA) or HistoMouse-Plus kit (Invitrogen), as per manufacturer's instruction. pS6-S235/236 antibody (#2211) was from Cell Signaling.

Immunostaining with c-Myc, GFAP and Neu N antibodies

Mice were sacrificed at age 17 days with euthanasia with CO_2 followed by immediate removal of brains and fixation in 2-methylbutane/dry ice bath. Brains were then embedded in tissue freezing medium and stored at −80°C (Tissue-Tek O.C.T. compound, Sakura Finetek Inc., Torrance, CA). Coronal sections were cut at a thickness of 10 μm and directly mounted on glass slides. Sections were stained with 1:1000 dilution of rabbit polyclonal anti-C-Myc peroxidase conjugate (# A5598, Sigma, St. Louis, MO), or double stained with 1:100 dilution of mouse monoclonal anti-C-Myc antibody (# 1667149, Roche Diagnostics), which recognizes the c-Myc tag sequence, and 1: 100 dilution of rabbit monoclonal antibody to neuronal marker (Neu N) (#ab177487, Abcam, Cambridge, MA) or 1:500 dilution of rabbit monoclonal antibody to glial fibrillary acidic protein (GFAP) (Clone G-A-5 cy3 conjugate, Sigma) in 0.1% Tween-20 in PBS overnight at 4°C, washed in PBS 3 × 10 min, and incubated for 1 h at room temperature with 1:1000 Alexa 488-conjugated goat anti-rabbit secondary antibody for single staining, or 1:1000 Alexa 647-conjugated goat anti-mouse and 1:1000 Alexa 555-conjugated goat anti-rabbit secondary antibodies (Life Technologies, Grand Island, NY) in 0.1% Tween-20 in PBS for double staining. After another 3 × 10 min washes in PBS, the slides were coverslipped using a frozen mounting media - ProLong® Gold Antifade Mountant with DAPI (# P36935, Life Technologies).

Neuronal cell measurements

H&E stained brain sections were imaged on a Zeiss Axiophot microscope, and images were captured from the retrosplenial granular and dysgranular cortex, primary and secondary motor cortex, and hindlimb and shoulder of prim somatosens regions in the left hemisphere of the cortex just above the lateral ventricles, the co-ordinates being the dorsal ventral −1.0 mm, lateral medial + 1.0 mm and anterior posterior −1.06 mm, as suggested by the

pathologist (A. S-R.), as these regions appeared to have the most notable differences in size of the neurons as compared among these sets of mice. Images were examined using Spot software, and the maximum diameter of all cells in the designated regions of cortex was measured in pixels using Photoshop (Adobe CS5) on the following number of cells for each group (3 animals per group): 26 mutant non-injected, 15 mutant injected with AAV-GFP vector, 19 mutant injected with AAV-hamartin vector, 19 normal- non-injected, 21 normal injected with AAV-GFP vector and 22 normal injected with AAV-hamartin vector.

Quantification and statistical analysis

Immunostaining density was quantitatively analyzed using Image J software (Fig 7). Survival curves were analyzed by the logrank (Mantel-Cox) test using GraphPad Prism software (GraphPad Software, Inc., La Jolla, CA). statistical significance was determined with $p < 0.05$ considered to be statistically significant (Fig. 5A) and Student T test was used for the analysis of weights of mice (Fig. 5B)

Results

Generation and characterization of the AAV-hamartin vector

The cDNA for human hamartin (TSC1-FLAGpcDNA; Murthy et al., 2000) was modified by replacing the FLAG tag with an in-frame c-Myc tag (10 amino acids) in the carboxy terminal and cloned into an AAV2 vector backbone under the CMV promoter (pAAV-CMV-hamartin-cmyc; Fig. 1). This plasmid, a parallel plasmid encoding GFP, and the original TSC1-FLAGpcDNA plasmid were transfected into 293T cells and cell lysates were resolved by SDS-PAGE and western blotting. Anti-human hamartin staining showed an appropriate 135 kDa band of the appropriate size expressed in the pAAV-hamartin-cmyc and TSC1-FLAGpcDNA transfected cells, with a faint band in AAV-GFP transfected and non-transfected cells (Fig. 2A) corresponding to low endogenous expression of hamartin in 293T cells. The packaged AAVrh8-hamartin-cmyc vector was also tested following infection of mouse neurons in culture. Western blot analysis showed expression of a c-Myc positive 135 kDa protein only in AAVrh8-hamartin-cmyc vector-infected neurons (Fig. 2B).

To evaluate whether the hamartin-cmyc fusion protein encoded in the AAV vector was functionally active, we evaluated the phosphorylation status of a human influenza hemagglutinin (HA) tagged version of HA-S6K in 293T cells transfected with different expression constructs, including the pAAV backbone (empty AAV vector), pAAV-CMV-hamartin-cmyc, pTSC2-FLAG, and pTSC1-FLAG together with pTSC2-FLAG, as previously described (Han et al., 2012). Protein lysates were immune precipitated using antibodies to HA and protein A-Sepharose. Both immune precipitates and original cell lysates were resolved by SDS-PAGE and western blotted using antibodies to pS6K (phosphorylated on threonine residue 389), a mixture of TSC2 and TSC1, and c-Myc (Fig. 3A). Phosphorylation of HA-S6K (ratio of pS6K to S6K) was markedly inhibited by co-expression of hamartin (TSC1) and tuberin (TSC2) when TSC1 was tagged with either FLAG or c-Myc, indicating functionality of the vector construct (Fig. 3B). This is consistent with the downstream inhibitory effects of the hamartin/tuberin complex on activity of

mTORC1 and consequent inhibition of phosphorylation of S6 kinase (Goncharova et al., 2002).

To assess whether the AAVrh8-hamartin vector could express hamartin *in vivo*, we injected 2×10^{10} g.c. vector into each ventricle in P0 pups. Both *Tsc1*^{cc}*SynIcre*$^{+}$ (mutant) and *Tsc1*^{cw}*SynIcre*$^{+}$ (normal) mice showed evidence of gene delivery to cells throughout the brain 18 days later as revealed by immunostaining for the c-Myc epitope (Fig. 4). Staining was seen in many cells in the cortex and striatum (Fig. 4A and B) and hippocampus (not shown), of vector-injected mutant mice, as well as in the cortex of vector-injected normal mice *cw*+ (Fig. 4C). The brains of non-injected mutant mice *cc*+ processed in parallel showed no c-Myc staining anywhere in the brain, as shown in the cortical region (Fig. 4D). Widespread staining for the transgene following ICV delivery of this AAV vector is consistent with that reported for the AAVrh8-GFP vector injected ICV in neonatal mouse brain (Broekman et al., 2006), as well as for other AAV serotypes (Gholizadeh et al., 2013). The transgene was expressed in both astrocytes and neurons as revealed by co-staining for c-Myc and GFAP or Neu N, respectively (Supplementary Fig. 1a and 1b).

Therapeutic effects of AAVrh8-hamartin vector in the Tsc1^{cc}SynIcre^{+} model

Litters composed of both *Tsc1*^{cc}*SynIcre*$^{+}$ (mutant) and *Tsc1*^{cw}*SynIcre*$^{+}$ (normal) pups were injected ICV with the AAVrh8-hamartin-cmyc at P0 as above. Mice were then followed and compared to control litters in which none of the pups were injected or injected with a control GFP vector. AAVrh8-hamartin-cmyc-injected mutant mice lived over twice as long as mutant mice that did not receive the vector injection (median survival of treated mice was 52 days vs. 22 days for non-injected mutants, $p<0.0001$, Fig. 5A, Table 1). All mouse groups, except the mutant non-injected ones, had similar starting weights at 18 days. The average weight of non-injected mutant animals compared to normal injected and non-injected was significantly ($p<0.01$) lower by 31.5% already at P18 (Fig. 5B). After that time point the non-injected mutant animals started dying and their weights were no longer determined. AAVrh8-hamartin-cmyc-injected mutant mice gained weight at a rate comparable to control mice up through postnatal day 46. In addition, the AAVrh8-hamartin-cmyc-treated mutant mice showed remarkably normal motor behavior until just before death. They were evaluated twice per week for tail position, tremors, hind limb clasping and hunched backs (kyphosis) with hamartin vector-injected mutants appearing very similar to normal control mice, while their non-treated mutant counterparts showed marked deterioration in all these parameters prior to early death (Table 1). No spontaneous seizures or changes in motor behavior were observed in the AAVrh8-hamartin-cmyc injected mutants (N=25) prior to death. Death presumably resulted from a chimeric state in the brain in which not all the *Tsc1*-null neurons were infected with AAVrh8-hamartin-cmyc vector and thus some aspects of abnormal neuronal function remained uncorrected. The rapid death could be explained acute respiratory failure caused by seizures, as hypothesized by Meikle et al. (2007), although in the current studies with reduced handling of mice, seizures were not observed.

Neuropathologic examination of the brains of mutant (non-injected or ICV-injected with a GFP vector), mutant injected with AAVrh8-hamartin-cmyc vector, and normal (non-injected or injected with hamartin-cmyc or GFP vectors) mice was performed at P18 to assess

expression and response to the hamartin or GFP vectors injected at P0. H&E staining of brains showed that the cell bodies of non-injected mutant cortical neurons were almost twice as wide in diameter in comparison to cortical neurons in non-injected control mice (Fig. 6), as observed previously (Meikle et al., 2008). Abnormal, enlarged neurons were also observed in the brain stem of mutant mice (Supplementary Fig. 2), which is a key center of respiratory control. The injection of the hamartin vector into mutant brains at P0 resulted in normalization of neuronal size in cortical regions for most neurons, with a significant difference in the neuronal mean diameter between the treated and non-injected mutant mice ($p < 0.00001$) and with no significant difference in the neuronal mean diameter between the treated mutant and the normal non-injected mice ($p<0.1$) (Fig. 6D). Importantly, injection of the same amount of a similar AAV vector encoding GFP or hamartin-cmyc did not change the size of neurons in the normal mice.

Second, immunostaining for pS6, which is elevated in the brains of mutant mice, was measured in different brain regions and increased staining was noted in the cortex, cerebellum and hippocampus in mutant non-injected mice as compared to AAVrh8-hamartin-cmyc injected mutant mice and normal controls (Fig. 7). Quantitative analysis of pS6 staining was carried out using Image J to evaluate differences in integrated pixel density (mean +/− SEM) in representative regions of the brains, including the entire cortex, cerebellum, hippocampus, olfactory lobes (not shown) and thalamus (not shown). Mutant non-injected mouse brains had $5.5 \times 10^7 \pm 1.1 \times 10^7$ pixels of pS6 staining (N=3); normal non-injected mouse brains, $2.4 \times 10^6 \pm 2.6 \times 10^5$ pixels (N=3); and AAVrh8-hamartin-cmyc injected mutant mouse brains, $1.0 \times 10^7 \pm 1.1 \times 10^6$ pixels (N=3). There was a statistically significant difference between mutant non-injected as compared to mutant injected brains ($p<0.05$), and no significant difference between AAVrh8-hamartin-cmyc injected mutant mouse brains and normal non-injected mouse brains ($p<0.1$). These values in integrated pixels are derived from the entire image shown in each panel and not the entire brain.

Discussion

Our studies indicate the remarkable therapeutic effectiveness on phenotype and survival of a single injection of an AAV-hamartin replacement vector into the brains of a mouse model with loss of Tsc1 in brain neurons starting during embryogenesis (Meikle et al., 2007 & 2008). Extensive therapeutic improvement was observed in normalization of brain neuropathology and motor behavior, as well as a marked increase in median survival. To our knowledge this is the first report of gene replacement therapy in a mouse model of TSC. It is important to compare the current findings with our previous studies using drug treatment in this same genetic model. We found that continuous treatment with either rapamycin or everolimus (RAD001) led to markedly extended median survival, and normalization of the behavioral phenotype and weight (Meikle et al., 2008). However, when drug treatment was terminated, the mutant mice rapidly declined and died. Hence, this new gene therapy approach of ICV AAV hamartin injection leads to a level of improvement in mutant mice that is similar to treatment with rapamycin, but provides extended benefit following a single vector injection. Of note, injection of the gene replacement vector in mouse brains at P0 is roughly equivalent to human brains at six months of fetal development (Clancy et al., 2007), and as such which would be inappropriate for the current state of clinical trials. However, a

single injection of AAV vector intravenous (i.v.) from birth to 9 month of age is part of an ongoing clinical trial for gene replacement in spinal motor atrophy (SMN) (clinical trials.gov). An upcoming clinical trial for AAV delivery into the intrathecal space of the spinal cord [which shares cerebral spinal fluid (CSF) with the cerebral ventricles] is also planned for SMN at early ages (Passini et al., 2014), so different time points and routes of vector injection should also be assessed in *Tsc* mouse models.

Several TSC tumors or related diseases, including renal angiomyolipoma, lymphangioleiomyomatosis, and subependymal giant-cell astrocytoma, have been shown to be responsive to treatment with mTOR inhibitors (sirolimus and everolimus) in randomized clinical trials (Bissler et al., 2013; Franz et al., 2013; McCormack et al., 2011). Furthermore, there is preliminary evidence that these medications may improve epileptic seizure control (Cardamone et al., 2014; Fukumura et al., 2014; Jülich and Sahin, 2014). However, mTOR is a critical and central regulator of anabolic processes throughout the body, and there is considerable concern that long term effects of treatment with these agents are unknown and may prove to be very significant. This issue is of particular concern in infants and young children for whom growth and development is obviously a critical process. For example, there is evidence that prenatal rapamycin treatment in mice can lead to significant toxicity in Tsc mutants (Anderl et al., 2011), and cause developmental delay and motor dysfunction in wild-type mice (Tsai et al., 2013). The potential side effects and necessity for long term treatment with mTOR inhibitors serves as an impetus to explore other therapeutic modalities.

In planning this gene therapy strategy, we have taken advantage of the observation that TSC1 and TSC2 together exert major effects on cell growth and brain cell function by regulating mTORC1 through their assembly in a complex that also includes TBC1D7 (Dibble et al., 2012). All components of this TSC protein complex are required for its proper function as a GTP-activating signaling protein to regulate the state of activation of RHEB, which then regulates the activity of mTORC1 (Garami et al., 2003; Zhang et al., 2003; Laplante and Sabatini, 2012). Hence, exogenous expression of TSC1, as effected here by infection with a gene therapy vector can serve to rescue normal levels of the TSC1-TSC2-TBC1D7 complex. Moderate over-expression of TSC1 should outstrip the supply of these other components, thus avoiding toxicity due to overactivity of the complex. This is important both for cells which have complete loss of TSC1, and for other cells without second allele loss which are undoubtedly also infected by the AAV virus and thus will express both endogenous hamartin and exogenous hamartin delivered by the AAV vector.

Overall, gene delivery to the brain is most efficient when carried out in the neonatal period and more efficient by direct ICV or intrathecal delivery than by IV delivery (for review see Maguire et al., 2014). Although our study used ICV AAV vector delivery, which is very efficient at transducing neurons and astrocytes throughout the brain (Broekman et al., 2006), other studies support the potential of IV delivery using select serotypes of AAV, which in addition to transduction of neurons and other cells in the brain also deliver the transgene to peripheral tissues, e.g. liver, kidney, lung and muscle (Foust et al., 2009; Zhang et al., 2011). Vascular delivery has the advantage of delivering the normal protein to peripheral tissues in the body, many of which are affected in TSC by loss of hamartin or tuberin function, while

also crossing the blood-brain barrier for delivery to the brain (McCown, 2010). Other methods of gene therapy delivery may also be considered, including: direct injection of the vector into epileptic foci in the brain to try to restore normal electrical activity; into tumor nodules, e.g. renal angiomyolipoma, to decrease cell size and abnormal growth; and into the cerebral ventricles to target subependymal nodules associated with hydrocephalus. Since both neurodevelopmental symptoms and seizures commonly occur during infancy in TSC, administration of an AAV TSC1 vector could be performed early for maximum benefit, possibly even neonatally, as is currently being done with AAV vectors in clinical trials for spinal muscular atrophy via both i.v. and intrathecal routes (Zanetta et al., 2014). It is also possible that older individuals with TSC1 with progressive lesions in the kidney or lung, for example, could benefit from vascular delivery of this gene replacement vector which, like rapamycin, should decrease cell size and growth, and hence volume of tumors resulting from loss of function of hamartin,

To our knowledge, this study is one of the first gene therapy protocols to target a tumor suppressor gene defect. TSC is inherited as an autosomal dominant disorder with germline mutations in one allele of either the TSC1 or TSC2 “tumor suppressor” gene. Disease phenotypes arise when different cell types take a “second hit” to the remaining normal allele which can happen in a variety of tissues during development or later in life. The severity of the disease relates in part to the frequency, timing and tissue type in which loss of TSC1 or TSC2 expression occurs. This results in variable phenotypes among patients with respect to different tissues being affected in different epochs, and with the full bodily extent of the disease being hard to predict and monitor. In addition to CNS involvement, which can include seizures, autism and intellectual disability, there are numerous dysfunctions in brain and peripheral tissues. For example, a number of tissues form benign tumors, e.g. subependymal giant cell astrocytomas in the brain (Lee et al., 2014), perivascular epithelioid tumors in the uterus (Celik et al., 2014), and spinal cord chordomas (Lee-Jones et al., 2004), as well as cellular overgrowths, e.g. angiomyolipomas of the smooth muscle in lung (Henske and McCormack, 2012) or kidney (Katabathina et al., 2012), with an increased predisposition to malignant renal cell carcinomas in the latter (Yang et al., 2014b). Thus, IV delivery may serve to reduce the size of lesions in different tissues throughout the body, as well as in the brain, and prevent potential conversion to malignancy.

Conclusion

These studies show that gene replacement of TSC1 (hamartin) to the brain in neonatal mice with loss of *Tsc1* in neurons can be remarkably effective in restoring neuronal morphology and motor behavior, as well as in improving lifespan, comparable to extended, ongoing treatment with rapamycin. Thus, gene therapy may have a useful application in TSC patients in several settings, including infancy for brain development and seizure improvement. AAV vector could be injected into the cerebral ventricles or intrathecal space throughout life to target brain lesions. In younger individuals IV injection might also transduce neurons in the brain, but would be most effective for peripheral lesions, with the potential to select specific AAV serotypes for tissue targeting. Vectors could also be injected directly into TSC related tumors or IV during later life to curtail proliferation of benign hamartomas in peripheral tissues, as well as to reduce their chances of becoming malignant. AAV vectors have been

shown to have low-to-no risk for gene therapy in human brain and other tissues in Phase 1 and 2 clinical trials (Maguire et al., 2014).

Supplementary Material

Refer to Web version on PubMed Central for supplementary material.

Acknowledgments

We thank Ms. Suzanne McDavitt for skilled editorial assistance; Michelle Forrestall Lee, Medical Photographer in Pathology Media Lab, MGH for the imaging training; Tao Qin, Laboratory Researcher in Department of Neurology, MGH for the Image J training; Mei Huan Lin for genotyping of the mice by MLPA analysis, DNA Core facility, Brigham and Women's Hospital, Boston, MA; Dr. Daniel Joyner, Department of Neurology, Alzheimer's Disease Research Unit, MGH, Charlestown, MA, for mouse neuronal cultures; Dr. Davide Gianni and MS-E, Vector Core, Gene Therapy Center, UMASS Medical School, Worcester, MA for AAV-hamartin vector packaging; and Ms. Danielle Morse and Dr. Bakhos Tannous, Vector Core, MGH, Charlestown, MA for AAV-GFP vector packaging. This work was supported by NIH/NINDS NS024279 (XOB, SP, AS-R, DJK); DOD Army Grant W81XWH-13-1-0076 (XOB and SP); NIH NINDSP30 NS045776 (XOB and SP); and the European Commission (DJK).

Abbreviations

AAV	adeno-associated virus
CBA	chicken beta actin
CMV	cytomegalovirus
CNS	central nervous system
CSF	cerebral spinal fluid
g.c	genome copies
GFAP	glial fibrillary acidic protein
HA-S6K	HA-S6 kinase
H&E	haematoxylin and eosin
HEK	human embryonic kidney
HA	human influenza hemagglutinin
HRP	horseradish peroxide
IHC	immunohistochemistry
IP	immunoprecipitation
i.v	intravenous
IV	intravascular
ICV	intracerebral ventricular
Neu N	neuronal nuclei

pS6	phospho-S6
RIPA	radio immunoprecipitation assay
SEGAs	subependymal giant cell astrocytomas
SMN	spinal motor atrophy
TSC	tuberous sclerosis complex

References

Anderl S, Freeland M, Kwiatkowski DJ, Goto J. Therapeutic value of prenatal rapamycin treatment in a mouse brain model of tuberous sclerosis complex. Hum Mol Genet. 2011; 20:4597–4604. [PubMed: 21890496]

Bissler JJ, Kingswood JC, Radzikowska E, Zonnenberg BA, Frost M, Belousova E, Sauter M, Nonomura N, Brakemeier S, de Vries PJ, Whittemore VH, Chen D, Sahmoud T, Shah G, Lincy J, Lebwohl D, Budde K. Everolimus for angiomyolipoma associated with tuberous sclerosis complex or sporadic lymphangioleiomyomatosis (EXIST-2): a multicentre, randomised, double-blind, placebo-controlled trial. Lancet. 2013; 381:817–824. [PubMed: 23312829]

Broekman ML, Comer LA, Hyman BT, Sena-Esteves M. Adeno-associated virus vectors serotyped with AAV8 capsids are more efficient than AAV-1 or -2 serotypes for widespread gene delivery to the neonatal mouse brain. Neuroscience. 2006; 138:501–510. [PubMed: 16414198]

Cardamone M, Flanagan D, Mowat D, Kennedy SE, Chopra M, Lawson JA. Mammalian target of rapamycin inhibitors for intractable epilepsy and subependymal giant cell astrocytomas in tuberous sclerosis complex. J Pediatr. 2014; 164:1195–1200. [PubMed: 24518170]

Carson RP, Van Nielen DL, Winzenburger PA, Ess KC. Neuronal and glia abnormalities in Tsc1-deficient forebrain and partial rescue by rapamycin. Neurobiol Dis. 2012; 45:369–380. [PubMed: 21907282]

Celık H, Kefelı M, Cetınkaya M, Yildiz L. Perivascular epithelioid cell tumor (PEComa) of the uterine cervix in a patient with tuberous sclerosis complex: A literature review. Turk Patoloji Derg. 2014; 11:1–5.

Clancy B, Finlay BL, Darlington RB, Anand KJ. Extrapolating brain development from experimental species to humans. Neurotoxicology. 2007; 28:931–937. [PubMed: 17368774]

Crino PB. Evolving neurobiology of tuberous sclerosis complex. Acta Neuropathol. 2013; 125:317–332. [PubMed: 23386324]

Dibble CC, Elis W, Menon S, Qin W, Klekota J, Asara JM, Finan PM, Kwiatkowski DJ, Murphy LO, Manning BD. TBC1D7 is a third subunit of the TSC1-TSC2 complex upstream of mTORC1. Mol Cell. 2012; 47:535–546. [PubMed: 22795129]

Feliciano DM, Lafourcade CA, Bordey A. Neonatal subventricular zone electroporation. J Vis Exp. 2013; 72 pii: 50197. doi: 10.3791/50197

Foust KD, Nurre E, Montgomery CL, Hernandez A, Chan CM, Kaspar BK. Intravascular AAV9 preferentially targets neonatal neurons and adult astrocytes. Nat Biotechnol. 2009; 27:59–65. [PubMed: 19098898]

Franz DN, Leonard J, Tudor C, Chuck G, Care M, Sethuraman G, Dinopoulos A, Thomas G, Crone KR. Rapamycin causes regression of astrocytomas in tuberous sclerosis complex. Ann Neurol. 2006; 59:490–498. [PubMed: 16453317]

Franz DN, Belousova E, Sparagana S, Bebin EM, Frost M, Kuperman R, Witt O, Kohrman MH, Flamini JR, Wu JY, Curatolo P, de Vries PJ, Whittemore VH, Thiele EA, Ford JP, Shah G, Cauwel H, Lebwohl D, Sahmoud T, Jozwiak S. Efficacy and safety of everolimus for subependymal giant cell astrocytomas associated with tuberous sclerosis complex (EXIST-1): a multicentre, randomised, placebo-controlled phase 3 trial. Lancet. 2013; 381:125–132. [PubMed: 23158522]

Fukumura S, Watanabe T, Takayama R, Minagawa K, Tsutsumi H. Everolimus treatment for an early infantile subependymal giant cell astrocytoma with tuberous sclerosis complex. J Child Neurol. 2014 Aug 19. Epub ahead of print.

Garami A, Zwartkruis FJ, Nobukuni T, Joaquin M, Roccio M, Stocker H, Kozma SC, Hafen E, Bos JL, Thomas G. Insulin activation of Rheb, a mediator of mTOR/S6K/4E-BP signaling, is inhibited by TSC1 and 2. Mol Cell. 2003; 11:1457–1466. [PubMed: 12820960]

Gholizadeh S, Tharmalingam S, Macaldaz ME, Hampson DR. Transduction of the central nervous system after intracerebroventricular injection of adeno-associated viral vectors in neonatal and juvenile mice. Hum Gene Ther Methods. 2013; 24:205–213. [PubMed: 23808551]

Goncharova EA, Goncharov DA, Eszterhas A, Hunter DS, Glassberg MK, Yeung RS, Walker CL, Noonan D, Kwiatkowski DJ, Chou MM, Panettieri RA, Krymskaya VP. Tuberin regulates p70 S6 kinase activation and ribosomal protein S6 phosphorylation. A role for the TSC2 tumor suppressor gene in pulmonary lymphangioleiomyomatosis (LAM). J Biol Chem. 2002; 277:30958–30967. [PubMed: 12045200]

Haddad LA, Smith N, Bowser M, Niida Y, Murthy V, Gonzalez-Agosti C, Ramesh V. The TSC1 tumor suppressor hamartin interacts with neurofilament-L and possibly functions as a novel integrator of the neuronal cytoskeleton. J Biol Chem. 2002; 277:44180–44186. [PubMed: 12226091]

Han S, Kim S, Bahl S, Li L, Burande CF, Smith N, James M, Beauchamp RL, Bhide P, DiAntonio A, Ramesh V. The E3 ubiquitin ligase protein associated with Myc (Pam) regulates mammalian/mechanistic target of rapamycin complex 1 (mTORC1) signaling in vivo through N- and C-terminal domains. J Biol Chem. 2012; 287:30063–30072. [PubMed: 22798074]

Henske EP, McCormack FX. Lymphangioleiomyomatosis - a wolf in sheep's clothing. J Clin Invest. 2012; 122:3807–3816. [PubMed: 23114603]

Jülich K, Sahin M. Mechanism-based treatment in tuberous sclerosis complex. Pediatr Neurol. 2014; 50:290–296. [PubMed: 24486221]

Katabathina VS, Garg D, Prasad SR, Vikram R. Cystic renal neoplasms and renal neoplasms associated with cystic renal diseases in adults: cross-sectional imaging findings. J Comput Assist Tomogr. 2012; 36:659–668. [PubMed: 23192202]

Krueger DA, Wilfong AA, Holland-Bouley K, Anderson AE, Agricola K, Tudor C, Mays M, Lopez CM, Kim MO, Franz DN. Everolimus treatment of refractory epilepsy in tuberous sclerosis complex. Ann Neurol. 2013; 74:679–687. [PubMed: 23798472]

Kwiatkowski, DJ.; Whittemore, VH.; Thiele, EA. Tuberous Sclerosis Complex: Genes, Clinical Features, and Therapeutics. Wiley-Blackwell; Weinheim, Germany: 2010.

Laplante M, Sabatini DM. mTOR signaling in growth control and disease. Cell. 2012; 149:274–293. [PubMed: 22500797]

Lee D, Cho YH, Kang SY, Yoon N, Sung CO, Suh YL. BRAF V600E mutations are frequent in dysembryoplastic neuroepithelial tumors and subependymal giant cell astrocytomas. J Surg Oncol. 2014 Oct 24. Epub ahead of print.

Lee-Jones L, Aligianis I, Davies PA, Puga A, Farndon PA, Stemmer-Rachamimov A, Ramesh V, Sampson JR. Sacrococcygeal chordomas in patients with tuberous sclerosis complex show somatic loss of TSC1 or TSC2. Genes Chromosomes Cancer. 2004; 41:80–85. [PubMed: 15236319]

Maguire C, Ramirex SH, Merkel SF, Sena-Esteves M, Breakefield XO. Gene therapy for the nervous system: challenges and new strategies. Neurotherapeutics. 2014; 11:817–839. [PubMed: 25159276]

Mao X, Fujiwara Y, Orkin SH. Improved reporter strain for monitoring Cre recombinase-mediated DNA excisions in mice. Proc Natl Acad Sci U S A. 1999; 96:5037–5042. [PubMed: 10220414]

McCormack FX, Inoue Y, Moss J, Singer LG, Strange C, Nakata K, Barker AF, Chapman JT, Brantly ML, Stocks JM, Brown KK, Lynch JP, Goldberg HJ, Young LR, Kinder BW, Downey GP, Sullivan EJ, Colby TV, McKay RT, Cohen MM, Korbee L, Taveira-DaSilva AM, Lee HS, Krischer JP, Trapnell BC. Consortium, N. I. o. H. R. L. D., Group, M. T. Efficacy and safety of sirolimus in lymphangioleiomyomatosis. N Engl J Med. 2011; 364:1595–1606. [PubMed: 21410393]

McCown TJ. Adeno-Associated Virus (AAV) Vectors in the CNS. Curr Gene Ther. 2011; 11:181–188. [PubMed: 21453285]

Meikle L, McMullen JR, Sherwood MC, Lader AS, Walker V, Chan JA, Kwiatkowski DJ. A mouse model of cardiac rhabdomyoma generated by loss of Tsc1 in ventricular myocytes. Hum Mol Genet. 2005; 14:429–435. [PubMed: 15601645]

Meikle L, Talos DM, Onda H, Pollizzi K, Rotenberg A, Sahin M, Jensen FE, Kwiatkowski DJ. A mouse model of tuberous sclerosis: neuronal loss of Tsc1 causes dysplastic and ectopic neurons, reduced myelination, seizure activity, and limited survival. J Neurosci. 2007; 27:5546–5558. [PubMed: 17522300]

Meikle L, Pollizzi K, Egnor A, Kramvis I, Lane H, Sahin M, Kwiatkowski DJ. Response of a neuronal model of tuberous sclerosis to mammalian target of rapamycin (mTOR) inhibitors: effects on mTORC1 and Akt signaling lead to improved survival and function. J Neurosci. 2008; 28:5422–5432. [PubMed: 18495876]

Murthy V, Haddad LA, Smith N, Pinney D, Tyszkowski R, Brown D, Ramesh V. Similarities and differences in the subcellular localization of hamartin and tuberin in the kidney. Am J Physiol Renal Physiol. 2000; 278:F737–F746. [PubMed: 10807585]

Nagabhushan Kalburgi S, Khan NN, Gray SJ. Recent gene therapy advancements for neurological diseases. Discov Med. 2013; 15:111–119. [PubMed: 23449113]

Passini MA, Bu J, Richards AM, Treleaven CM, Sullivan JA, O'Riordan CR, Scaria A, Kells AP, Samaranch L, San Sebastian W, Federici T, Fiandaca MS, Boulis NM, Bankiewicz KS, Shihabuddin LS, Cheng SH. Translational fidelity of intrathecal delivery of self-complementary AAV9-survival motor neuron 1 for spinal muscular atrophy. Hum Gene Ther. 2014; 25:619–630. [PubMed: 24617515]

Prabhakar S, Goto J, Zhang X, Sena-Esteves M, Bronson R, Brockmann J, Gianni D, Wojtkiewicz GR, Chen JW, Stemmer-Rachamimov A, Kwiatkowski DJ, Breakefield XO. Stochastic model of Tsc1 lesions in mouse brain. PLoS One. 2013; 8:e64224. [PubMed: 23696872]

Samaranch L, Salegio EA, San Sebastian W, Kells AP, Foust KD, Bringas JR, Lamarre C, Forsayeth J, Kaspar BK, Bankiewicz KS. Adeno-associated virus serotype 9 transduction in the central nervous system of nonhuman primates. Hum Gene Ther. 2012; 23:382–389. [PubMed: 22201473]

Schuster DJ, Dykstra JA, Riedl MS, Kitto KF, Belur LR, McIvor RS, Elde RP, Fairbanks CA, Vulchanova L. Biodistribution of adeno-associated virus serotype 9 (AAV9) vector after intrathecal and intravenous delivery in mouse. Front Neuroanat. 2014; 8:42. [PubMed: 24959122]

Sena-Esteves M, Tebbets JC, Steffens S, Crombleholme T, Flake AW. Optimized large-scale production of high titer lentivirus vector pseudotypes. J Virol Methods. 2004; 122:131–139. [PubMed: 15542136]

Simonato M, Bennett J, Boulis NM, Castro MG, Fink DJ, Goins WF, Gray SJ, Lowenstein PR, Vandenberghe LH, Wilson TJ, Wolfe JH, Glorioso JC. Progress in gene therapy for neurological disorders. Nat Rev Neurol. 2013; 9:277–291. [PubMed: 23609618]

Stoothoff W, Jones PB, Spires-Jones TL, Joyner D, Chhabra E, Bercury K, Fan Z, Xie H, Bacskai B, Edd J, Irimia D, Hyman BT. Differential effect of three-repeat and four-repeat tau on mitochondrial axonal transport. J Neurochem. 2009; 111:417–427. [PubMed: 19686388]

Tsai PT, Greene-Colozzi E, Goto J, Anderl S, Kwiatkowski DJ, Sahin M. Prenatal rapamycin results in early and late behavioral abnormalities in wildtype C57BL/6 mice. Behav Genet. 2013; 43:51–59. [PubMed: 23229624]

Uhlmann EJ, Wong M, Baldwin RL, Bajenaru ML, Onda H, Kwiatkowski DJ, Yamada K, Gutmann DH. Astrocyte-specific TSC1 conditional knockout mice exhibit abnormal neuronal organization and seizures. Ann Neurol. 2002; 52:285–296. [PubMed: 12205640]

Yang B, Li S, Wang H, Guo Y, Gessler DJ, Cao C, Su Q, Kramer J, Zhong L, Ahmed SS, Zhang H, He R, Desrosiers RC, Brown R, Xu Z, Gao G. Global CNS Transduction of Adult Mice by Intravenously Delivered rAAVrh.8 and rAAVrh.10 and Nonhuman Primates by rAAVrh.10. Mol Ther. 2014a; 22:1299–1309. [PubMed: 24781136]

Yang P, Cornejo KM, Sadow PM, Cheng L, Wang M, Xiao Y, Jiang Z, Oliva E, Jozwiak S, Nussbaum RL, Feldman AS, Paul E, Thiele EA, Yu JJ, Henske EP, Kwiatkowski DJ, Young RH, Wu C. Renal cell carcinoma in tuberous sclerosis complex. Am J Surg Pathol. 2014b; 38:895–909. [PubMed: 24832166]

Yeung RS. Lessons from the Eker rat model: from cage to bedside. Curr Mol Med. 2004; 4:799–806. [PubMed: 15579026]

Zanetta C, Nizzardo M, Simone C, Monguzzi E, Bresolin N, Comi GP, Corti S. Molecular therapeutic strategies for spinal muscular atrophies: current and future clinical trials. Clin Ther. 2014; 36:128–140. [PubMed: 24360800]

Zeng LH, Xu L, Gutmann DH, Wong M. Rapamycin prevents epilepsy in a mouse model of tuberous sclerosis complex. Ann Neurol. 2008; 63:444–453. [PubMed: 18389497]

Zhang H, Yang B, Mu X, Ahmed SS, Su Q, He R, Wang H, Mueller C, Sena-Esteves M, Brown R, Xu Z, Gao G. Several rAAV vectors efficiently cross the blood-brain barrier and transduce neurons and astrocytes in the neonatal mouse central nervous system. Mol Ther. 2011; 19:1440–1448. [PubMed: 21610699]

Zhang Y, Gao X, Saucedo LJ, Ru B, Edgar BA, Pan D. Rheb is a direct target of the tuberous sclerosis tumour suppressor proteins. Nat Cell Biol. 2003; 5:578–581. [PubMed: 12771962]

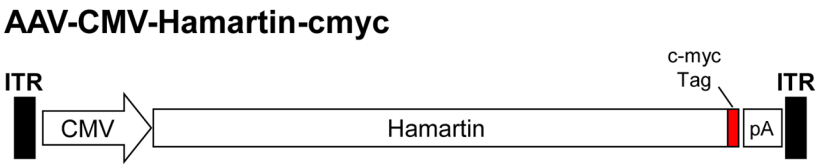

Figure 1. AAV-CMV-hamartin-cmyc construct

AAV cassette in AVV2-LTR backbone in which human hamartin cDNA is under control of the CMV promoter and tagged with a c-Myc peptide at the C-terminal. pA refers to polyadenylation signal.

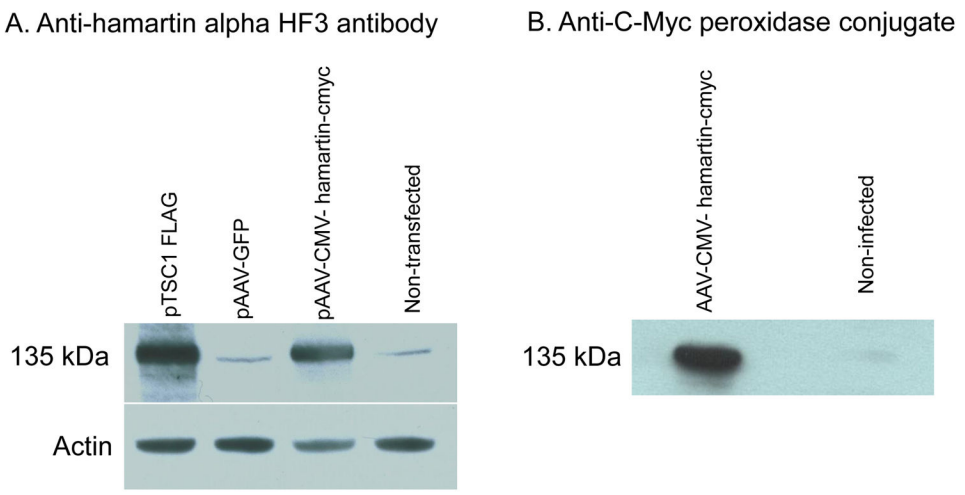

Figure 2. PAGE/western blot

A. *Hamartin antibody staining.* 293T cells were transfected with AAV-CMV-hamartin-cmyc, AAV-GFP or hamartin (TSC1FLAG) cDNA expression plasmids. Seventy-two h later, the cells were lysed, proteins resolved by PAGE and western blots carried out using alphaHF3 antibody to human hamartin. Beta-actin antibody was used as a control for loading. **B**. *C-myc antibody staining*. Mouse neurons in culture were infected with AAVrh8-CMV-hamartin-cmyc vector or not infected, media was changed after 24 h, and then 72 h later the cells were lysed and PAGE/western blotting was carried out staining with c-Myc antibodies.

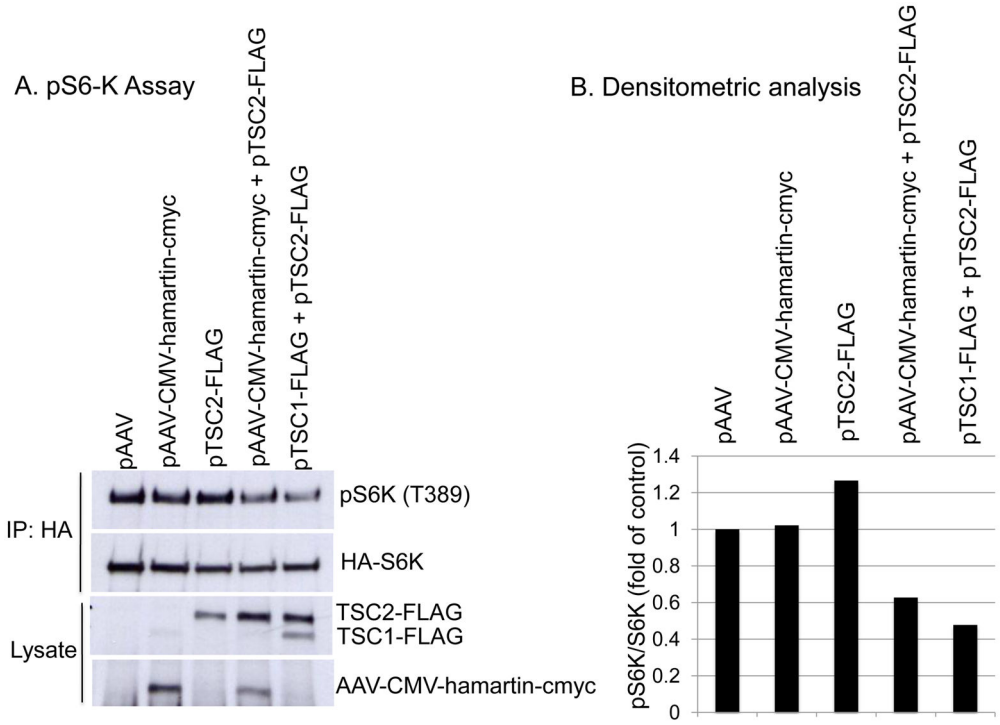

Figure 3. The Myc-tagged, TSC1 AAV construct (AAV-CMV-hamartin-cmyc) inhibits mTORC1 signaling

The HA-tagged S6K (HA-S6K) was transfected into 293T cells along with the indicated constructs including AAV-CMV-hamartin-cmyc. **A**. Anti-HA immunoprecipitates or cell lysates from the transfected cells were resolved by SDS-PAGE and probed on western blots with anti-HA, anti-pS6K (T389), anti-FLAG, or anti-Myc antibodies. **B**. Band intensities from a representative western blot were quantitated using scanned images by densitometer (Bio-Rad). The levels of pS6K(T389) were normalized against HA-S6K levels and graphed as a fold of the control group (pAAV).

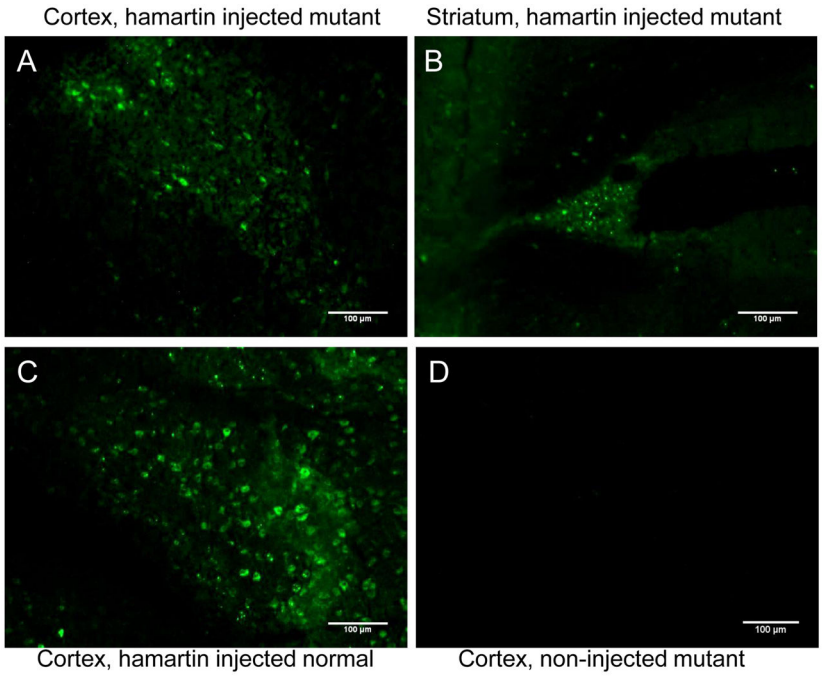

Figure 4. Immunostaining with c-Myc antibody

Pups were injected at P0 ICV in both ventricles (2×10^{10} g.c. in 2 µl in each ventricle with an AAV vector encoding hamartin-cmyc or non-injected. On day 18, the brains of the injected mutant and normal mice, as well as non-injected mutant mice were harvested and stained for the c-Myc tag indicating the expression of the hamartin transgene in various brain regions. C-Myc staining was evident in the (**A**) cortex and (**B**) striatum in hamartin vector-injected mutant mouse brains, and in the (**C**) cortex of hamartin vector-injected normal mice. (**D**) No staining was detected in the non-injected mutant mouse brains. Magnification = 10X; scale bar = 100 µm.

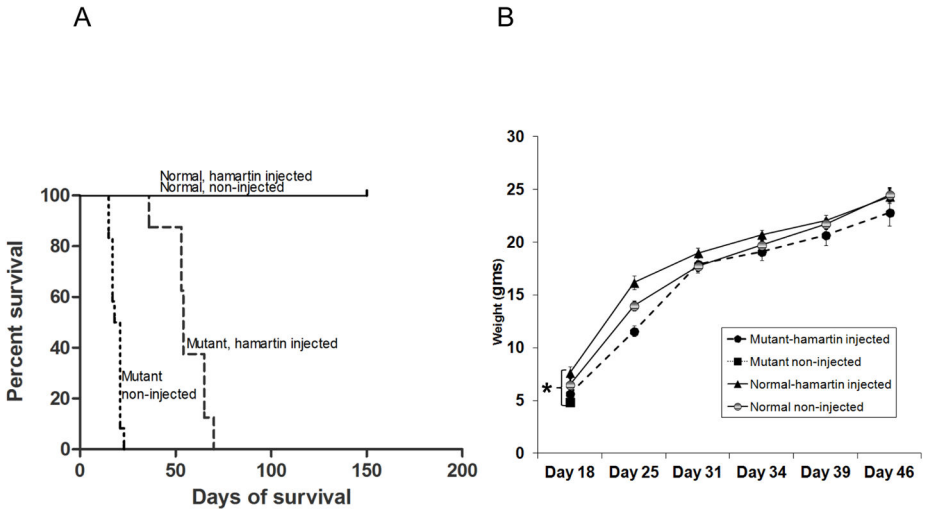

Figure 5. Gene therapy for mice which lack hamartin in neurons in the brain

Tsc1SynCre^{cw++} mice were crossed with Tsc1^{cc-} mice to obtain offspring which were either null (mutants, Tsc1SynCre^{cc+}) or heterozygous for wild-type (normals, Tsc1SynCre^{cw+}) hamartin in neurons in the brain. At P0, littermates were injected ICV in both ventricles (2×10^{10} g.c. in 2 μl into each ventricle) with an AAV vector encoding hamartin or were left non-injected. Mice were monitored for (**A**) survival data, shown as Kaplan-Meier curves for non-injected normal mice (N=11), hamartin vector-injected normals (N=11), non-injected mutants (N=12) and hamartin vector-injected mutants (N=10). There was a highly significant difference between non-injected and vector injected mutants, $p<0.0001$ (Mantal-Cox test, graph pad prism). (**B**) Weight of mice was also tracked over a 3 month period, with the weight of non-injected mutants at P18 being significantly lower than for the other mouse groups at this time point ($p<0.009$; T-test) [after which non-injected mutant mice started dying].

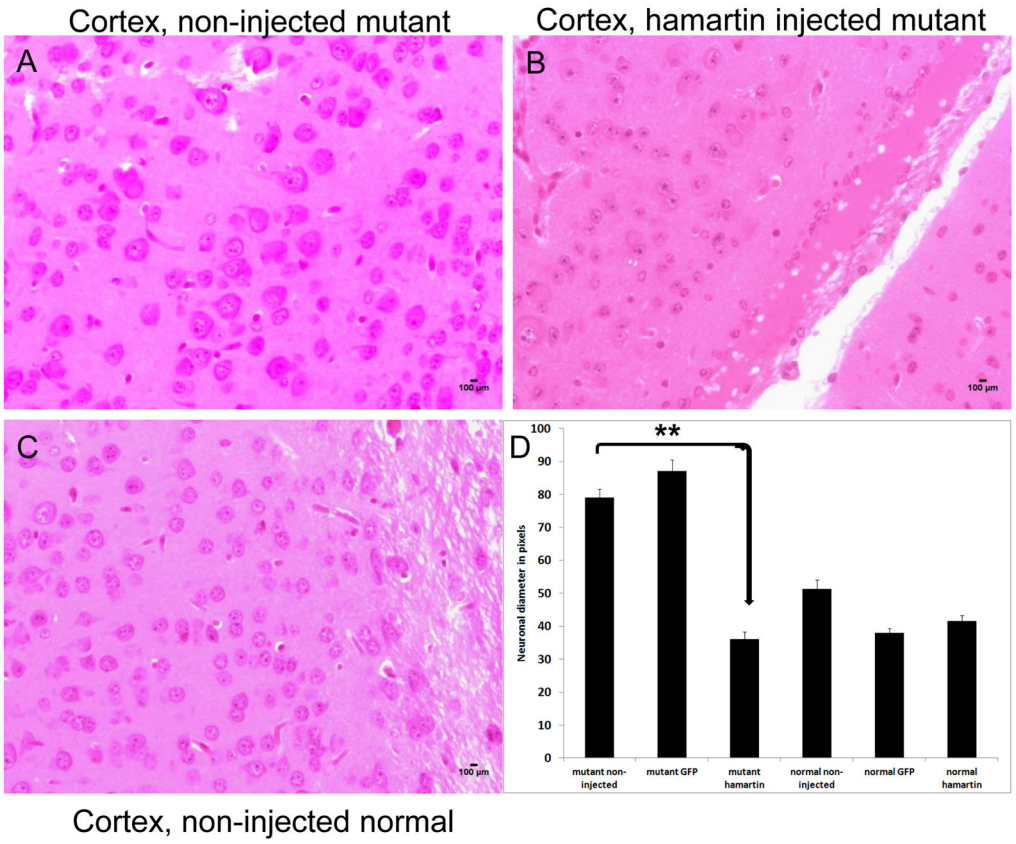

Figure 6. H&E staining of brain sections and measurement of neuronal diameter

A–C: At P18, staining of brains with H&E shows that cell bodies of neurons in the cortical region right above the lateral ventricles in the non-injected mutants (**A**) and GFP vector-injected mutants (not shown) appeared considerably larger than those in hamartin vector-injected mutants (**B**) or non-injected controls (**C**), with representative images shown from the non-injected mutant mice, hamartin vector-injected and control non-injected. Magnification = 40X; scale bar = 100 µm. (**D**) Neural cells in the periventricular region of the brains of hamartin and GFP vector-injected, as well as non-injected mice (P18) were randomly selected and the widest diameter of stained cell bodies was measured from several fields in 15–26 cells for each group with 3 animals per group. Neural cells in the GFP vector-injected and non-injected brains of the mutants were 2-fold greater in diameter, as compared to hamartin vector-injected mutants or controls, shown as mean ± SEM (**$p < 0.00001$), with no statistically significant difference between mutant hamartin vector-injected and the three controls (normal non-injected, normal GFP vector-injected and normal hamartin vector-injected).

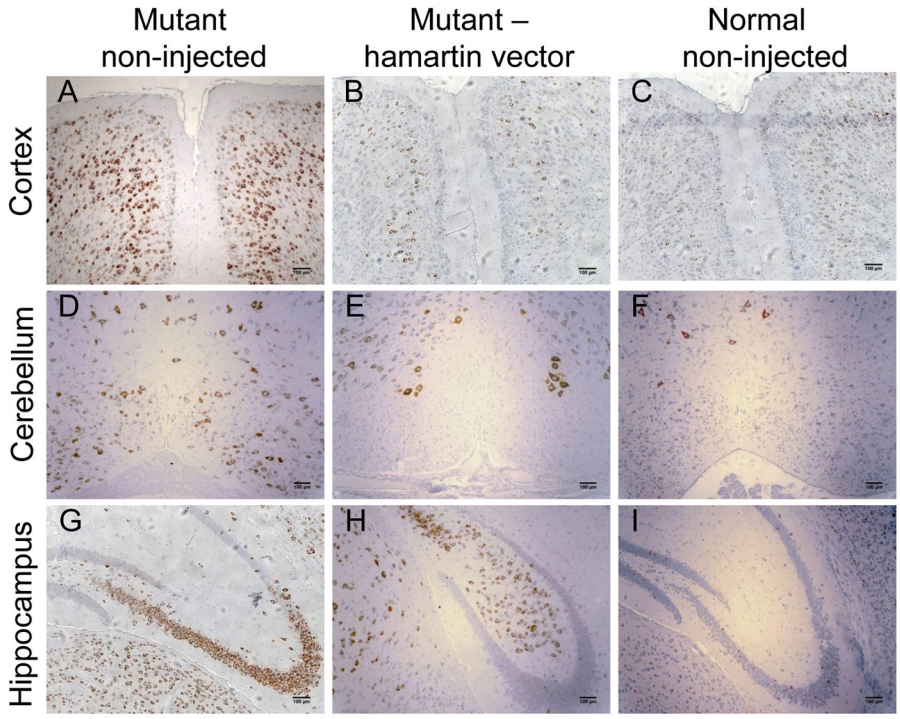

Figure 7. pS6 staining in brains of hamartin vector-injected Tsc1SynCre^{cw+} and Tsc1SynCre^{cc+} mice

The pups of cross mating between Tsc1SynCre^{cw++} and Tsc1Syn^{cc-} mice were injected ICV at P0 with either an AAVrh8-CMV-hamartin-cmyc (N=6) or AAVrh8-GFP (N=6) vector at a concentration of 2 μl (10^{10} g.c/ul) per ventricle or non-injected (N=6). Injected and non-injected mice (N=4) were sacrificed at P18 and evaluated for pS6 levels by immunocytochemistry. Mutant non-injected and GFP vector-injected (latter not shown) brains had more intense pS6 positivity in cortex, cerebellum, hippocampus, olfactory lobes (not shown), thalamus (not shown) and basal ganglia (not shown) when compared with the mutants injected with hamartin vector (intermediate staining) and normal mice non-injected (low staining) or injected with hamartin or GFP vectors (not shown). Magnification = 20X; scale bar = 100 μm.

Table 1

Behavioral analysis of normal, Tsc1-neuronal null and Tsc1-neuronal null/AAV-hamartin injected mice

Non-injected mutants[a] (*cc*+) #	**Days of survival[b]**	**Weight (gms) at 18 days[c]**	**Tail position[d]***	**Whole body tremor[d]***	**Hindleg clasping[d]***	**Kyphosis[d]***
7	15	5.8 ± 0.1	3	4	1	1
11	17	5.3 ± 0.1	3	4	1	1
8	21	5.6 ± 0.1	2	3	1	1
Hamartin injected mutants (*cc*+) #	**Days of survival**	**Weight (gms) at 18 days**	**Tail position***	**Whole body tremor***	**Hindleg clasping***	**Kyphosis***
9	36	6.7 ± 0.1	1	0	0	0
9	53	6.9 ± 0.1	1	0	0	0
7	70	7.1 ± 0.1	1	0	0	0
Hamartin injected normal (*cw*+) #	**Days at sacrifice**	**Weight (gms) at 18 days**	**Tail position***	**Whole body tremor***	**Hindleg clasping***	**Kyphosis***
10	36	7.2 ± 0.1	0	0	0	0
17	53	7.2 ± 0.1	0	0	0	0
12	70	7.3 + 0.1	0	0	0	0

[a] Mutant refers to *Tsc1neuronal null* mice with genotype *Tsc1SynCre*$^{cc+}$, and normals to controls with genotype *Tsc1SynCre*$^{cw+}$. Injected and non-injected refer to whether or not pups were injected ICV with the AAVrh8-CMV-hamartin-cmyc vector at P0. Number of animals (#) tested per group in each experiment is indicated.

[b] All animals were sacrificed at the same time points as the injected mutants when comparing the brains by histopathology.

[c] Average values for weight of animals in each group at P18.

[d] Behavioral measures assessed on P18, including average score values for tail position, tremor, clasping and kyphosis scores (assessed as described in the Methods). Tremor and tail position were scored on 0–5 and 0–3 scales (over a range of normal to abnormal), respectively. Clasping and kyphosis were assessed on a binary 0 (absent) or 1 (present) scale. *Note.* All the neurologic scores were consistent in each group (*).